

Water molecules in the cannabinoid receptor 2 binding site crucially impact the discovery of novel ligands

Magdalena M. Scharf^{1,†}, Morgan Scott-Dennis^{2,3}, Leire Borrega-Roman^{2,3}, Franziska N. Z. Giese¹, Darya Plevako^{2,3}, David A. Sykes^{2,3}, Dmitry B. Veprintsev^{2,3,*}, and Peter Kolb^{1,*}

¹Institute of Pharmaceutical Chemistry, University of Marburg, Marburg, Germany

²Division of Physiology, Pharmacology and Neuroscience, School of Life Sciences, University of Nottingham, Nottingham, UK

³Centre of Membrane Proteins and Receptors (COMPARE), University of Birmingham and University of Nottingham, Midlands, UK

[†]Current address: Department of Physiology and Pharmacology, Karolinska Institutet, Stockholm, Sweden

*To whom correspondence should be addressed:
dmitry.veprintsev@nottingham.ac.uk, peter.kolb@uni-marburg.de

January 20, 2025

Abstract

The cannabinoid receptor 2 (CB₂R) is of considerable therapeutic and scientific interest. Hence, the discovery of novel molecules that target and modulate this receptor, ideally selectively over its closest relative, the cannabinoid receptor 1, is of great importance. In this study, we aimed to discover novel ligands targeting the CB₂R using large library *in silico* docking screens. However, since the CB₂R binding site is difficult to target with *in silico* methods due to its hydrophobic nature, we used a variety of screening approaches, including the placement of water molecules in predicted water sites of the receptor binding site, and screening against multiple docking setups and receptor conformations. We systematically evaluated these different approaches to support future screens to the CB₂R and other receptors. In the present work, each setup contributed different ligands of varying intrinsic activities, leading to an overall improved hit rate compared to that of a single screen. Of the novel ligands of the CB₂R discovered and experimentally confirmed in this study, one series features high-affinity ligands with a previously undescribed scaffold.

Introduction

With experimental structure determination of G protein-coupled receptors (GPCRs) becoming routine in recent years, structure-based approaches for ligand identification have also increased in frequency. Depending on the type of ligand and the desired ligand features, different strategies have been employed by us and others. This has included (1) docking to individual receptors to tailor selectivity (1, 2); (2) docking to distinct receptor conformations to tailor efficacy (3) and; (3) docking to single wild-type and mutant receptors, with and without explicit water molecules, to predict poses (i.e. the combination of molecule conformation and spatial orientation in the binding pocket) of known ligands. (4, 5)

In this work, we targeted the human cannabinoid receptor 2 (CB₂R) with large-scale docking calculations. This GPCR is highly expressed in immune tissues such as the spleen and lymph nodes, and on white blood cells. (6–8) Additionally, the CB₂R is found in peripheral tissues, including the liver (9, 10), kidney (11, 12), gastrointestinal tract (13), and on certain bone cells including osteoblasts and osteoclasts. (14) The CB₂R is also highly expressed in activated microglia and brain macrophages, which defend against injury or infection. (15) It is furthermore implicated in cardiovascular, gastrointestinal, liver, kidney, lung, and neurodegenerative diseases, having a function in tissue injury, repair, and inflammation. (16) Ongoing research indicates that the CB₂R plays a crucial role in regulating neuronal function in the central nervous system, with expression increasing with inflammation in diseases like cancer and neurodegenerative disorders. (17, 18)

Activation of the CB₂R, mainly via G_{ai/o} protein coupling, is often protective. This has led to the development of CB₂R drug discovery programs, with an emphasis on developing agonists exhibiting selectivity for the CB₂R over the CB₁R. (19) However, in certain disease states, CB₂R immunosuppressive effects may exacerbate tissue damage and potentially promote cancer progression, meaning that CB₂R inverse agonists and antagonists might offer therapeutic benefits in these scenarios. (20–23)

Despite the wealth of pre-clinical data suggesting a role for the CB₂R in various disease states, there is still a lack of successfully trialled molecules on the market. Currently, only dronabinol (synthetic THC) and nabilone (a synthetic substance similar to THC) are approved by the FDA, and are used to treat chemotherapy-induced nausea and emesis.

We thus aimed to enrich the landscape of existing CB₂R ligands, which involved setting up our ligand screens in order to maximise the number of identifiable ligands. Since the CB₂R ligand binding pocket is fairly hydrophobic, we experimented with the addition of water molecules to it. In addition, we used different active and inactive receptor conformations, with the objective of analysing the efficacies of the emerging ligands. Predicted hits were

confirmed in membrane- and cell-based ligand-binding and signalling assays to assess their affinity and pharmacological activity. We identified ligands with high hit rates and high affinity for the CB₂R, and interestingly these resulted from docking calculations to several docking setups. A high-affinity ligand series based on a scaffold unprecedented for CB₂R ligands, featured a ligand that remarkably had an affinity on par with the reference ligand SR-144,528. In order to provide possible guidelines for future screens, we then evaluated whether each set of novel CB₂R ligands could have been found from any of the other docking calculations.

Results and Discussion

This study aimed to identify novel ligands for the CB₂R through docking screens of large molecular libraries and by employing diverse docking setups. In particular, the use of water molecules placed in the orthosteric binding site was explored as a means to improve the results of docking calculations and screens. To support the docking results, compounds selected from the *in silico* screens were characterised in cell-based assays to determine their affinity and functional effect on the CB₂R, as well as its closest relative, the CB₁R. Finally, the results from both docking calculations and pharmacological characterisation were combined for an additional analysis of the used docking approach and the usefulness of diversified docking setups in such studies.

Receptor preparation and water site prediction

Since the binding pocket of the CB₂R is mostly hydrophobic, it is considerably more difficult to obtain meaningful molecule poses from docking calculations to this receptor compared to similar, but more hydrophilic binding sites, as recently discussed by Stasiulewicz *et al.* (24). This problem emerged in our case when docking a set of 33 known ligands to three experimental structures of the CB₂R (PDB IDs 5ZTY, 6PT0 and 6KPF). Overall, high energy values of the scoring function, unfavourable orientations of the molecules in the binding site, as well as stranded hydrogen bond donors, were observed in these docking calculations. Thus, the usefulness of these docking setups for prospective docking screens was doubtful.

In particular, we noted an unsatisfied hydrogen bond acceptor upon redocking of CB₂R ligand AM10257. In principle, the acceptor pointed in the direction of a potential donor from S285^{7x38} (superscripts indicate numbering according to GPCRdb nomenclature, (25)) but at too large a distance (4.5 Å; Supplementary Figure S1), which suggested a water molecule. Therefore, we tried including water molecules in the ligand binding site of the CB₂R during docking calculations. Firstly, docking calculations were performed in which the single water molecule resolved in the binding site of the structure with PDB ID 5ZTY was maintained. However, we found this water molecule to be out of reach of the molecules in the ligand test set. The binding site was then explored further for polar interaction sites by applying SEED and docking small molecular fragments into the binding pocket of structure 5ZTY. Specifically, the location of the polar fragments methanol and ethanol close to S285^{7x38} indicated a potentially relevant water site that would allow bridging interactions between S285^{7x38} and the ligand AM10257 in the structure 5ZTY (Supplementary Figure S1). Indeed, a similar water-mediated interaction and a water network, including S^{7x38} and H^{2x65}, have previously also been suggested for the CB₁R (26, 27), supporting our assumption.

This potential water binding site – as well as others within the binding pocket – was then explored further using two water site prediction softwares, namely MOE’s Solvent Analysis tool and OpenEye’s SZMAP. To narrow down the choice of potential water sites to be considered further for docking calculations, four different criteria were applied: (1) water sites had to be located within the binding site and in reach of potential ligands; (2) favourable energy scores for the predicted water sites were preferred; (3) water sites predicted by more than one of the prediction tools were considered more likely and; (4) overlapping predictions of water sites between the different structures used were considered as a stronger signal. Notably, both prediction softwares predicted water sites in the same location as the crystallised water in structure 5ZTY (Supplementary Figure S1). In addition, both prediction softwares also predicted water sites close to S285^{7x38} and overlapping with the placement of methanol and ethanol by SEED. At this position, a water molecule could potentially mediate interactions to a ligand.

In addition to using different CB₂R structures and varying the placement of water molecules, an additional computational strategy was to use an alternative template ligand taken from a CB₁R structure. This chemical structure is more similar to the phytocannabinoid THC than the ligand present in the CB₂R structure, and was used for a docking setup where the protein was still based on structure 5ZTY.

Evaluation of the diverse docking setups was conducted using docking calculations of the set of known ligands and visually inspecting the resulting molecule poses, including their overall orientation and potential polar interactions (Supplementary Table S1 contains a complete list of setups and Supplementary Figure S2 shows all predicted water sites and template ligands used). This analysis revealed an overall increase of the number of hydrogen bonds in the water-containing compared to the water-free docking setups (Supplementary Table S2). This increase in the number of hydrogen bonds was partly due to polar interactions between ligands and water molecules, partly due to altered docking poses because of the presence of the water molecules. Furthermore, the overall pose quality increased for water-containing compared to the corresponding water-free docking setups. Moreover, similarity between the scaffold of the template ligand (used as a basis for the “matching spheres” in the docking calculations) and the scaffold of a docked molecule positively impacted pose quality. Finally, for each of the experimental structures, the docking setups yielding the largest numbers of favourable molecule poses were used for the subsequent docking screens: S285^{7x38}, 5ZTY_{AM841} (truncated AM841 as alternative template ligand and water molecule close to S285^{7x38}), 6PT0 (no water), 6PT0_{H₂O} (water molecule close to S285^{7x38}) and 6KPF_{H₂O} (two water molecules close to S285^{7x38} and L182^{ECL2}, respectively).

Docking screen

The ZINC15 drug-like subset (> 10 million molecules) was docked to the five docking setups described in the previous section using DOCK3.7 (Figure 1). Furthermore, the ranking lists resulting from these docking calculations were re-ranked to favour molecules that ranked well in docking calculations to all active conformations of the receptor (6PT0 and 6KPF). This was done as a means to enrich agonists over antagonists, which has worked previously in our hands. (3) The top 500-ranked molecule poses of each of the ranking and re-ranking lists were then evaluated visually. Additionally, an ECFP4 Tanimoto similarity filter (with a cutoff of 0.45), removing molecules similar to previously described ligands of the CB₂R as extracted from the ChEMBL database, was applied to the top 2000 molecules of each ranking list. This on average removed 78% of the molecules from each of the lists. The top 500 molecule poses of each resulting filtered list were then also inspected visually. Moreover, we wondered how much each of the lists of top 500 molecules differed, i.e. what the added value of each docking setup and each re-ranking to the overall performance of the campaign was. As shown in Supplementary Table S3, the overlap for most of the individual ranking lists (namely Ranking lists 1-5 in Figure 1) is single-digit and only 15 and 17 molecules for Ranking lists 4 vs. 5 and 2 vs. 3, respectively. The same is true for the “no water” vs. “water” setups: the overlap for corresponding pairs is 17 molecules or less and only marginally higher compared to other pairings (Supplementary Table S3).

Finally, 29 molecules were selected and purchased to be pharmacologically characterised. We note that occurrence of a compound in multiple lists was not a criterion of the likelihood with which a compound was selected for testing.

Pharmacological characterisation

The affinity of all 29 selected molecules was determined at the CB₂R using TR-FRET binding assays (Table 1, Supplementary Table S4 and Supplementary Figure S4). To assess the selectivity of each ligand, although not part of the prediction, analogous assays were conducted at the CB₁R (Supplementary Figure S5). Compounds MS009, MS021 and MS022 showed the highest affinity towards the CB₂R with pK_i values of 6.54 ± 0.08 , 7.63 ± 0.20 and 7.70 ± 0.10 , respectively (Figure 2A). Notably, compound MS018 was selective towards the CB₁R over the CB₂R in binding assays (approximately 20-fold selectivity).

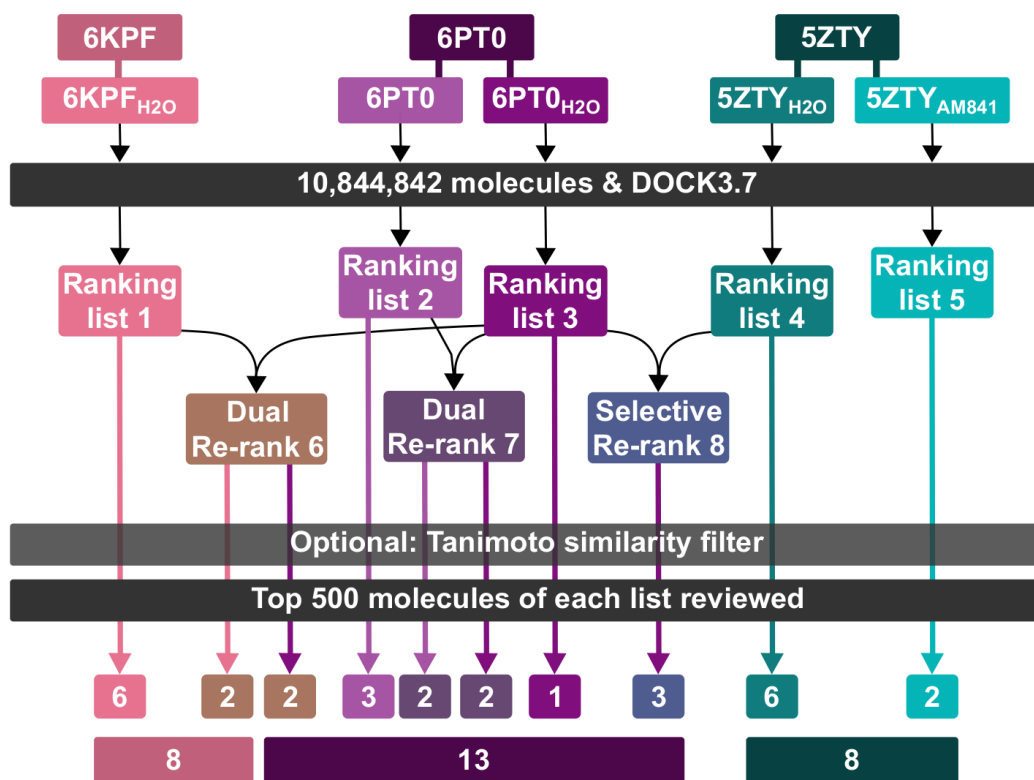


Figure 1: Docking scheme as employed in the present study. The PDB IDs of the CB₂R structures as well as the docking setups are indicated at the top. Numbers in the small squares indicate how many molecules were picked based on the ranking list in the corresponding colour and the docking setup indicated by the arrow colour. Larger boxes at the bottom indicate number of molecules selected for each CB₂R structure.

Table 1. Structures and affinities of all tested compounds with a $pK_i > 5$ at the CB₂R. pK_i -values are listed as mean \pm SEM for the CB₂R. n specifies the number of independent biological replicates. All percentage inhibition values can be found in Supplementary Table S5.

| ID | Structure | CB ₂ R | | CB ₁ R | |
|-------|-----------|-------------------|-----|-------------------|-----|
| | | pK_i | n | pK_i | n |
| MS022 | | 7.70 ± 0.10 | 14 | ND | 3 |

Continuation of Table 1.

| ID | Structure | CB ₂ R | | CB ₁ R | |
|-------|-----------|----------------------------|----------|---------------------|----------|
| | | pK _i | <i>n</i> | pK _i | <i>n</i> |
| MS021 | | 7.63 ± 0.20 | 14 | ND | 2 |
| MS009 | | 6.54 ± 0.08 | 14 | ND | 2 |
| MS003 | | 5.60 ± 0.11 ^{app} | 5 | NB | 2 |
| MS010 | | 5.49 ± 0.09 | 5 | 5.2 | 2 |
| MS013 | | 5.33 ± 0.39 ^{app} | 3 | 39.1 ± 0.5% @ 30 μM | 2 |
| MS019 | | 5.27 ± 0.32 ^{app} | 3 | 4.65 ^{app} | 2 |
| MS018 | | 5.19 ± 0.48 ^{app} | 3 | 6.45 ^{app} | 2 |
| MS002 | | 5.13 ± 0.06 ^{app} | 5 | 5.16 ^{app} | 2 |
| MS011 | | 5.11 ± 0.09 ^{app} | 3 | 4.78 ^{app} | 2 |

Continuation of Table 1.

| ID | Structure | CB ₂ R | | CB ₁ R | |
|--------------------------|-----------|-------------------|----------|-------------------|----------|
| | | pK _i | <i>n</i> | pK _i | <i>n</i> |
| Reference ligands | | | | | |
| SR-144,528 | | 8.43 ± 0.09 | 6 | NT | |
| Rimonabant | | NT | | 8.93 ± 0.2 | 3 |

NT: Not Tested. NB: Not Binding. ND: Not Determined due to insufficient number of data points and assay interference. ^{app}Apparent pK_i; this denomination is used when the concentration-response curve does not reach a plateau at the highest concentration and the inflection point has been determined under the assumption that such a plateau will eventually be reached.

The three highest-affinity compounds were characterised further using three functional assays: (1) mini-G_{si} recruitment and (2) β-arrestin recruitment assays, which both measure recruitment of transducer proteins to the receptor; and (3) the G_i-CASE biosensor assay, which is used to determine G protein activation (Supplementary Figure S3 shows schemes of the assays). While two of the compounds (MS021 and MS022) acted as partial agonists in all three functional assays, one compound (MS009) acted as an antagonist/inverse agonist (Supplementary Table S6 and Figure 2B-D). Consistent with receptor conformation, the two partial agonists resulted from docking calculations to an active CB₂R conformation, while the antagonist was selected from the docking calculation to an inactive CB₂R conformation.

Secondary screen

The three molecules displaying the highest affinities towards the CB₂R (MS009, MS021, MS022) were selected for a subsequent analogue search. Two additional molecules, MS005 and MS025, were selected to establish a baseline for the improvement of the top ligands, and results are described in the Supplementary Information. For each of these molecules, a library of similar molecules was derived and docked to the docking setup the parent molecule had been extracted from. The only exception were the docking calculations of the libraries based on MS021, for which the parent molecule (i.e. MS021 itself) was used as the template ligand to increase sampling around poses where the core scaffold was placed in a manner similar to the parent compound. The resulting molecule poses from each of the docking calculations were then inspected visually, and six to seven molecules were selected for each parent compound to be purchased and pharmacologically characterised.

For all derivative compounds the affinity towards the CB₂R and the CB₁R was then determined (Table 2; Figure 3A; Supplementary Figures S6; S7). Several compounds from the three series (based on MS009, MS021, MS022) had an affinity towards the CB₂R that

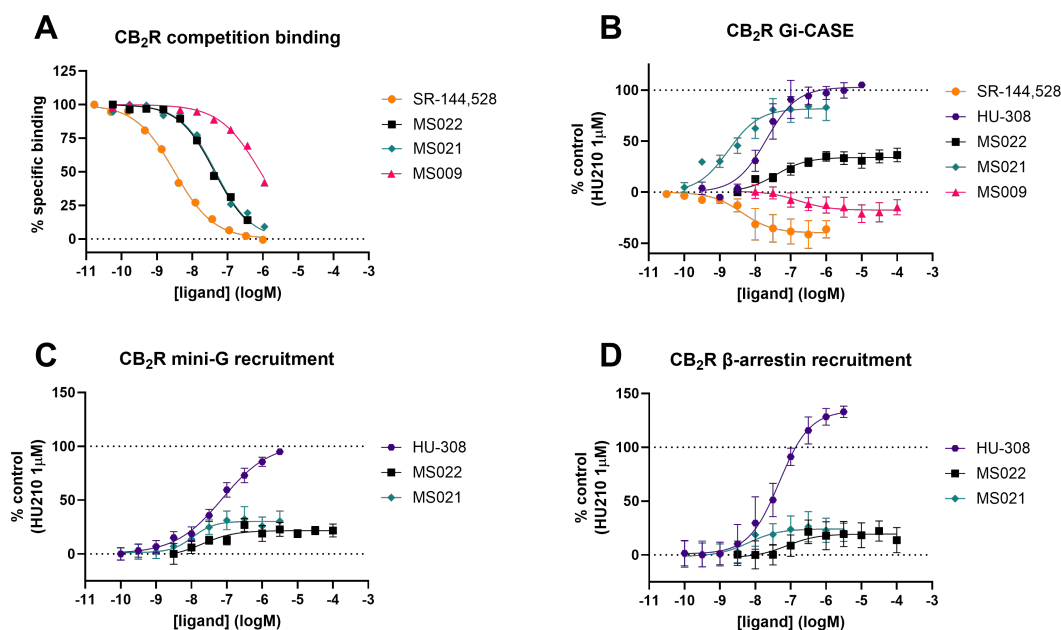


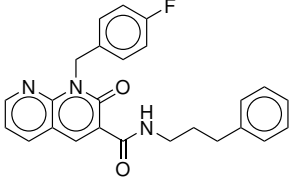
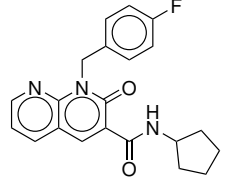
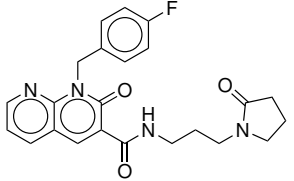
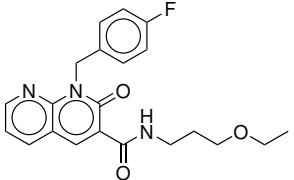
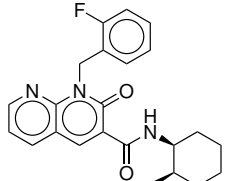
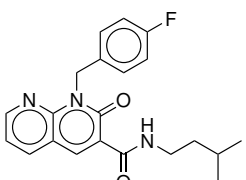
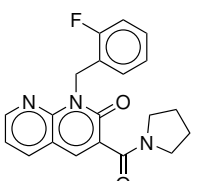
Figure 2: Assay results for the three compounds with the highest affinity from the primary docking screen (MS009, MS021 and MS022). A: Competition binding assay to measure compound affinity at the CB₂R for the three compounds and reference SR-144,528. B: G_i protein activation determined using the G_i-CASE sensor for the three compounds, SR-144,528 (inverse agonist) and HU-308 (full agonist). An increase in signal above zero indicates agonism, a decrease below zero inverse agonism. C, D: Recruitment of (C) mini-G_{si} and (D) β-arrestin to the receptor upon stimulation with agonists MS021 or MS022 or reference agonist HU-308. B-D: Values are normalised to the response of reference agonist HU-210. Binding data are exemplary measures from 3 or more experiments. Functional data is mean ± SEM of 3 or more measurements. Assay principles are depicted in Supplementary Figure S3.

was in the same range as the parent compounds. All compounds from the series based on MS021 and MS022, as well as three compounds from the series based on MS009, were characterised further using mini-G_{si} and β-arrestin recruitment as well as the G_i-CASE sensor (Supplementary Tables S7; S8).

Table 2. Structures and affinities of all compounds from the secondary screen based on MS009, MS021 and MS022. pK_i values are listed as mean \pm SEM for the CB₂R, or as percentage inhibition \pm SEM (mean \pm SD for the CB₁R) at the given concentration. n specifies the number of independent biological replicates. All percentage of inhibition values can be found in Supplementary Table S5.

| ID | Structure | CB ₂ R | | CB ₁ R | |
|----------------------|-----------|-----------------------------------|-----|-----------------------------------|-----|
| | | pK_i | n | pK_i | n |
| Parent: MS009 | | | | | |
| MS201 | | $15.3 \pm 2.4 \% @ 3 \mu\text{M}$ | 3 | ND | 2 |
| MS202 | | $6.16 \pm 0.04^{\text{app}}$ | 3 | 5.42^{app} | 2 |
| MS203 | | $5.96 \pm 0.04^{\text{app}}$ | 3 | ND | 2 |
| MS204 | | $5.77 \pm 0.18^{\text{app}}$ | 3 | ND | 2 |
| MS205 | | $35.4 \pm 4.3 \% @ 3 \mu\text{M}$ | 3 | $23.7 \pm 1.0 \% @ 3 \mu\text{M}$ | 2 |
| MS206 | | $41.5 \pm 6.0 \% @ 1 \mu\text{M}$ | 3 | ND | 2 |
| Parent: MS021 | | | | | |

Continuation of Table 2.

| ID | Structure | CB ₂ R | | CB ₁ R | |
|----------------------|---|----------------------------|----------|---------------------|----------|
| | | pK _i | <i>n</i> | pK _i | <i>n</i> |
| MS401 |  | 7.16 ± 0.10 | 4 | 18.3 ± 6.7% @ 10 μM | 3 |
| MS402 |  | 8.14 ± 0.22 | 5 | ND | 3 |
| MS403 |  | 6.04 ± 0.09 | 5 | NB | 3 |
| MS404 |  | 6.62 ± 0.11 | 4 | NB | 3 |
| MS405 |  | 7.28 ± 0.13 | 5 | 18.7 ± 5.5% @ 3 μM | 3 |
| MS406 |  | 7.75 ± 0.11 | 4 | 20.4 ± 8.5% @ 3 μM | 3 |
| MS407 |  | 5.00 ± 0.08 ^{app} | 5 | 7.7 ± 4.7% @ 30 μM | 3 |
| Parent: MS022 | | | | | |

Continuation of Table 2.

| ID | Structure | CB ₂ R | | CB ₁ R | |
|-------|-----------|----------------------------|----------|----------------------------|----------|
| | | pK _i | <i>n</i> | pK _i | <i>n</i> |
| MS501 | | 6.27 ± 0.09 ^{app} | 4 | 17.5 ± 15.7% @ 3 μM | 3 |
| MS502 | | 8.30 ± 0.22 | 5 | ND | 2 |
| MS503 | | 7.12 ± 0.14 | 4 | 16.1 ± 10.5% @ 10 μM | 3 |
| MS504 | | 7.55 ± 0.10 | 4 | 5.59 ± 0.05 ^{app} | 3 |
| MS505 | | ND | | ND | |
| MS506 | | 6.06 ± 0.14 ^{app} | 4 | 14.1 ± 6.1% @ 3 μM | 3 |

NB: Not Binding. ND: Not Determined due to insufficient number of data points and assay interference. ^{app} Apparent pK_i; this denomination is used when the concentration-response curve does not reach a plateau at the highest concentration and the inflection point has been determined under the assumption that such a plateau will eventually be reached.

The compound series based on MS021 contained 7 compounds, of which 2 compounds

had a higher or similar affinity and 5 compounds had a lower affinity compared to the parent compound (MS021 $pK_i = 7.63 \pm 0.20$; Table 2). Compounds MS402 ($pK_i = 8.14 \pm 0.22$) and MS406 ($pK_i = 7.75 \pm 0.11$) displayed the highest measured CB₂R affinities of the MS021 series (Figure 3A). Moreover, the entire series of compounds acted as partial agonists in the functional assays (Supplementary Table S7). Within this compound series, MS404 was the most and MS407 the least efficacious compound, respectively, while MS402 was the most and MS403 the least potent compound, respectively (Figure 3B-D; Supplementary Figure S8).

The compound series based on MS022 contained 6 compounds, of which 1 compound could not be pharmacologically characterised due to assay interference. Of the remaining 5 compounds, 2 showed a higher or similar affinity, and 3 a lower affinity towards the CB₂R compared to the parent molecule (MS022 $pK_i = 7.70 \pm 0.10$; Table 2). The 2 compounds with the highest affinity within the MS022 series were MS502 ($pK_i = 8.30 \pm 0.22$) and MS504 ($pK_i = 7.55 \pm 0.10$) (Figure 3A). Remarkably, the affinity of MS502 is in a similar range to that of the reference compound SR-144,528 ($pK_i = 8.43 \pm 0.09$). All compounds acted as either weak partial agonists or antagonists at the CB₂R in the functional assays (Table S7). Among the compounds of this series, MS501 and MS503 had the highest efficacy, while MS504 was the most potent compound (Figure 3B-D and Supplementary Figure S8), especially in the G_i protein activation assay using the G_i-CASE sensor.

The compound series based on the antagonist/inverse agonist MS009 resulted in 1 compound with a similar affinity compared to the parent (MS009 $pK_i = 6.54 \pm 0.08$; 47.0 % @ 1 μ M) and 5 compounds with lower affinities (Table 2; Supplementary Figure S6). The 3 compounds with the highest affinity, i.e. MS202, MS203 and MS206 were tested for inverse agonism of G_i protein-mediated signalling based on the parent compound properties. Indeed, all 3 compounds acted as antagonists/inverse agonists with varying potency and efficacy values (Supplementary Table S8; Figure 4).

Molecule poses

All of the three highest-affinity compounds MS009, MS021 and MS022, as well as their daughter compounds, were predicted to have their aromatic moieties placed in the receptor sub-pocket delimited by TM3, TM5 and TM6 (Figure 5). As known from experimental CB₂R structures, this sub-pocket is occupied by several (e.g. WIN55,212-2 or AM10257), but not all known CB₂R ligands (e.g. not by classical and bicyclic cannabinoids). Located at the edge of this sub-pocket is W258^{6x48}, which is the “toggle switch” residue involved in the activation of CB receptors and other class A GPCRs. (19, 28, 29) Blocking the rotational freedom of this residue is associated with antagonism and inverse agonism. Consistent with

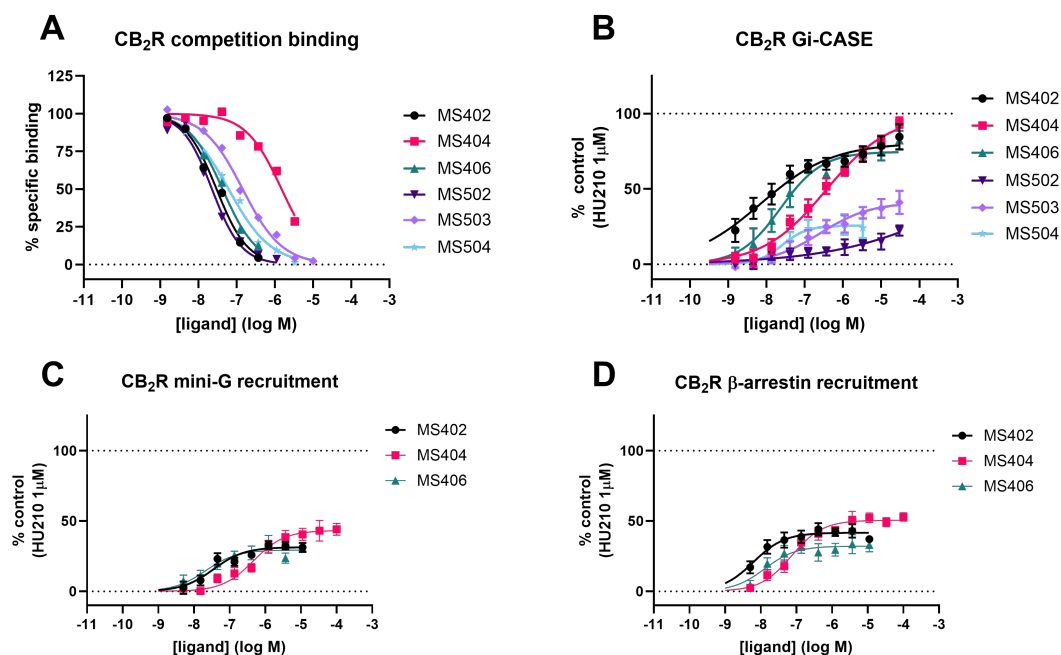


Figure 3: Assay results for select compounds from the secondary docking screen. A: Competition binding assay to measure compound affinity at the CB₂R. B: G_i protein activation determined using the G_i-CASE sensor. All shown compounds acted as partial agonists in reference to the full agonist HU-210, except for MS502 which acted as an antagonist. C, D: Recruitment of mini-G_{si} (C) and β-arrestin (D) to the receptor upon ligand stimulation and in reference to the response of the full agonist HU-210. While MS420, MS404 and MS406 acted as partial agonists, MS503 and MS504 induced only barely measurable recruitment of mini-G_{si} and β-arrestin and are not shown here. Binding data are exemplary measures from 3 or more experiments. Functional data is mean ± SEM of 3 or more measurements. Assay principles are depicted in Supplementary Figure S3.

this hypothesis, the core ring system of antagonist/inverse agonist MS009, as well as its daughter compounds MS201-MS206, stretched towards W258^{6x48}, similar to AM10257 in PDB ID 5ZTY (Supplementary Figure S9). In contrast, partial agonists MS021 and MS022 did not extend quite as far towards W258^{6x48} in their predicted binding poses.

During the initial optimisation of the docking setups, it was observed that introducing water molecules into the binding site generally improved molecule poses for the set of reference ligands, by enabling more polar interactions and better placement of aromatic moieties to form aromatic interactions. This can also be evaluated for the compounds selected from the primary screen. When comparing the poses of the ten binding molecules (ligands with affinities to the CB₂R with pK_i>5) between the original docking and the corresponding water-free/water-containing docking, the poses improved for the majority of molecules when

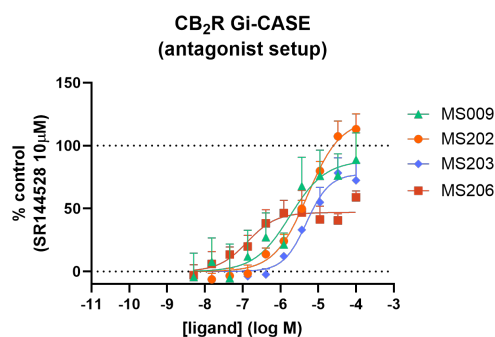


Figure 4: Measurement of inverse agonism using the G_i-CASE sensor assay in antagonist mode for MS009 and its derivatives MS202, MS203 and MS206. All compounds acted as inverse agonists with varying potency and efficacy in comparison to the reference inverse agonist SR-144,528. Data shown is mean \pm SEM of 3 or more measurements.

introducing a water molecule. Improved poses could, for example, be seen for the high-affinity compounds MS021 and MS022, while the pose of MS009 was very similar in both docking setups.

Generally, the introduction of a water molecule never led to a worsening of the pose, although this observation might be skewed since the majority of molecules were picked from docking calculations to water-containing setups. A more direct comparison can be made for the molecules selected from the docking calculations to 6PT0 and 6PT0_{H₂O} as the respective water-free and water-containing setups. In this case, it could be observed that the poses of each molecule selected from one of these setups was either similar in both setups or better in the water-containing setup, irrespective of the setup the molecule was originally picked from.

A direct interaction with the water molecule could be observed for 48% of the molecules selected in the primary screen. In general, ligands seemed to be more likely to interact with the water molecule than the non-binding or low-affinity molecules, with 70% of binding molecules, but only 37% of non-binding or low-affinity molecules interacting with a water molecule (for all molecules picked from 6PT0, the pose in 6PT0_{H₂O} was considered for this analysis). These results point towards a positive effect on docking results and ligand hit rates of carefully placed water molecules in the binding site. However, both the small sample size and the variety of docking setups the molecules were chosen from should also be acknowledged when interpreting these results.

Additional discussions of molecule poses can be found in the Supplementary Information.

Novelty of hit compounds

To evaluate the novelty of all tested compounds and discovered ligands, the ECFP4 Tanimoto similarity (T_c) between each compound and previously reported ligands of the CB₂R and the CB₁R as retrieved from ChEMBL, was calculated (Supplementary Tables S10 and S11). Tanimoto similarities of all compounds from the primary screen to known ligands of the CB₂R ranged from 0.26 to 0.58, plus a single compound with a particularly high similarity of 0.83 (Supplementary Figure S10). Of the ten compounds with a $pK_i > 5$, five had a $T_c \leq 0.40$ and seven a $T_c \leq 0.45$ to known ligands of the CB₂R, two had a T_c of 0.49 and one a T_c of 0.83. Of the three compounds with the highest affinities towards the CB₂R, two (MS009 and MS022) had a T_c of 0.42 to ligands of the CB₂R. However, the third compound (MS021) resembled a previously published compound series, which was reflected in a T_c of 0.83 and is largely based on a shared core scaffold. (30) Consequently, the compound series based on this hit molecule (MS401-MS407) also exhibited high T_c values of 0.52 to 0.96 to previously published ligands of the CB₂R. As this similarity was only noted after selection and characterisation of all compounds, it does therefore not impact the conclusions drawn here. However, the compounds from the other two high-affinity series based on MS009 and MS022 can be considered as mostly novel with T_c values of 0.4 to 0.5 and of 0.35 to 0.42, respectively. In particular, the latter series holds promise for further development with several compounds with high affinity for the CB₂R and low structural resemblance to previously published ligands of either the CB₂R or the CB₁R. The compound from this series with the highest affinity to the CB₂R, MS502, has a T_c value of 0.42 to known CB₂R and CB₁R ligands. For most of the tested molecules, the T_c values to ligands of the CB₂R and the CB₁R are in a comparable range, reflecting the overlapping molecular space of CB₂R and CB₁R ligands.

Hit rate

Based on the affinity of the characterised compounds, different hit rates can be defined. From the primary screen, 3 compounds out of 29 (10% of the 29 molecules) showed an affinity towards the CB₂R with $pK_i > 6$, 5 compounds (17%) had a $pK_i > 5.4$ and 10 compounds (34%) had a $pK_i > 5$. In addition, the hit rate can be evaluated based on the ranking lists the compounds were selected from (Supplementary TableS12). From the ranking lists of the original docking calculations, a total of 18 molecules were picked, of which 5 ligands (28%) were obtained. The remaining 11 molecules were picked from the re-ranked lists, yielding 5 ligands (45%). Notably, hit rates comparing the different docking setups or comparing water-containing with water-free setups were not calculated due to the small sample size for

the individual setups. A description of the hit rates from the secondary screen can be found in the Supplementary Information.

Docking data analysis

The molecules from the primary screen were picked from a variety of docking setups and re-rankings. Hence, one can analyse from which ranking lists compounds were selected, how much overlap exists between the molecule sets selected from each of the ranking lists and whether there are specific trends for ligands with a $pK_i > 5$ versus non-binding or low affinity molecules (Figure 6 and Supplementary Data).

We evaluated the degree of overlap between (1) water-free and corresponding water-containing docking setups as well as (2) re-ranking and corresponding original ranking (Figure 6A). In the first case, no overlap between water-containing and corresponding water-free setups exists up to the top 1000 ranked molecules of the ranking lists, and with only 6 overlapping molecules out of 29 (21 %) in the top 5000. In the second case, the overlap of molecules that could have been picked from both original ranking *and* corresponding re-ranking (including only the re-rankings that were used in the docking screen) is, as expected, low with 0 (top 500; 0 %), 6 (top 1000; 21 %) and 13 (top 5000; 45 %) molecules overlapping out of the 29 molecules, respectively.

This can be compared with whether any of the picked molecules could have been found from any other docking setup or ranking list (including re-rankings and water-free re-dockings) based on a compound's rank. When inspecting the top 500 molecules of all ranking lists, only 5 molecules out of 29 (17 %) could have been found in another ranking. As expected, this number increases when considering increasing portions of the ranking lists, to 14 (top 1000; 48 %) and 20 molecules (top 5000; 69 %), respectively.

While this evaluation gives insights into the general overlap between the different ranking lists, it can also be evaluated whether differences in overlap for the found ligands with a $pK_i > 5$ ("ligands"), in comparison to the non-binding/low affinity molecules in the various different ranking lists, exist (Figure 6B).

When comparing the overlap between the top 1000 ranked molecules of re-ranking list and corresponding original ranking lists, a slightly higher value can be observed for the ligands in comparison to the non-binding/low affinity molecules. While the overlap is 21 % (6/29) for all picked molecules, it is 30 % (3/10) for the ligands and 16 % (3/19) for the found non-binding/low affinity molecules. A similar trend can be observed when evaluating how many of the molecules could have been found in the top 1000 of any of the other ranking lists. While this overlap was 48 % (14/29) when including all of the picked molecules, this

value is higher with 70% (7/10) for the ligands and lower for the non-binding/low affinity molecules with only 37% (7/19).

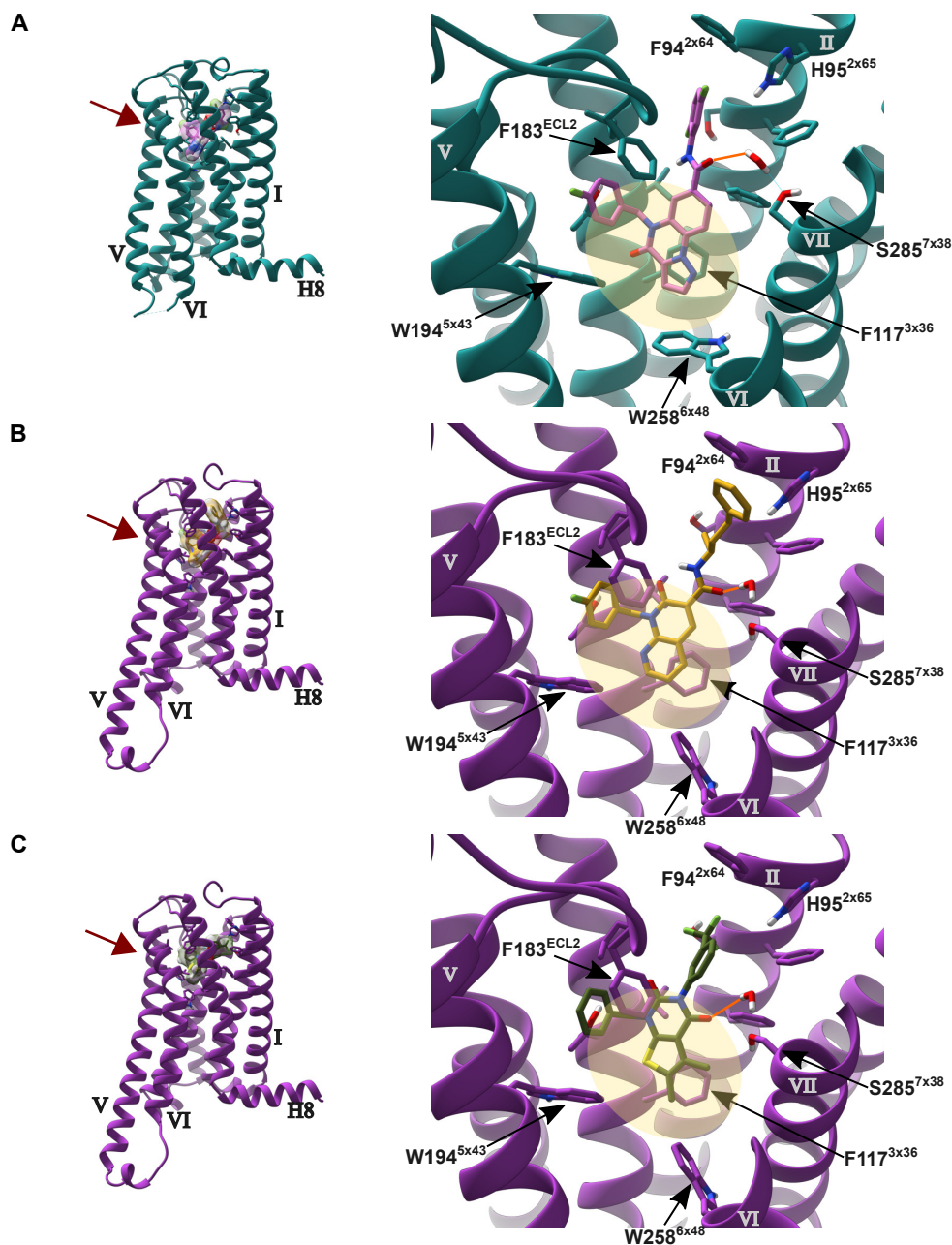


Figure 5: Predicted binding poses of the three highest-affinity hits from the primary screen. A: Docking pose of MS009 (pink) in docking setup 5ZTY_{AM841}. B: Docking pose of MS021 (gold) in docking setup 6PT0_{H2O}. C: Docking pose of MS022 (olive) in docking setup 6PT0_{H2O}. On the left, a side view of the CB₂R with the respective ligand in the orthosteric binding site is shown. The red arrow indicates the view point for the right panel. For all three ligands, the placed water molecule is involved in a polar interaction with the ligand, as indicated by an orange line. TM numbers (roman numerals) and names of important residues in the binding site are labelled. Pale yellow ovals indicate the receptor sub-pocket spanned by TM3, TM5 and TM6. Note that TM6 and TM7 are partially hidden in the right panel to allow a better view on the ligand.

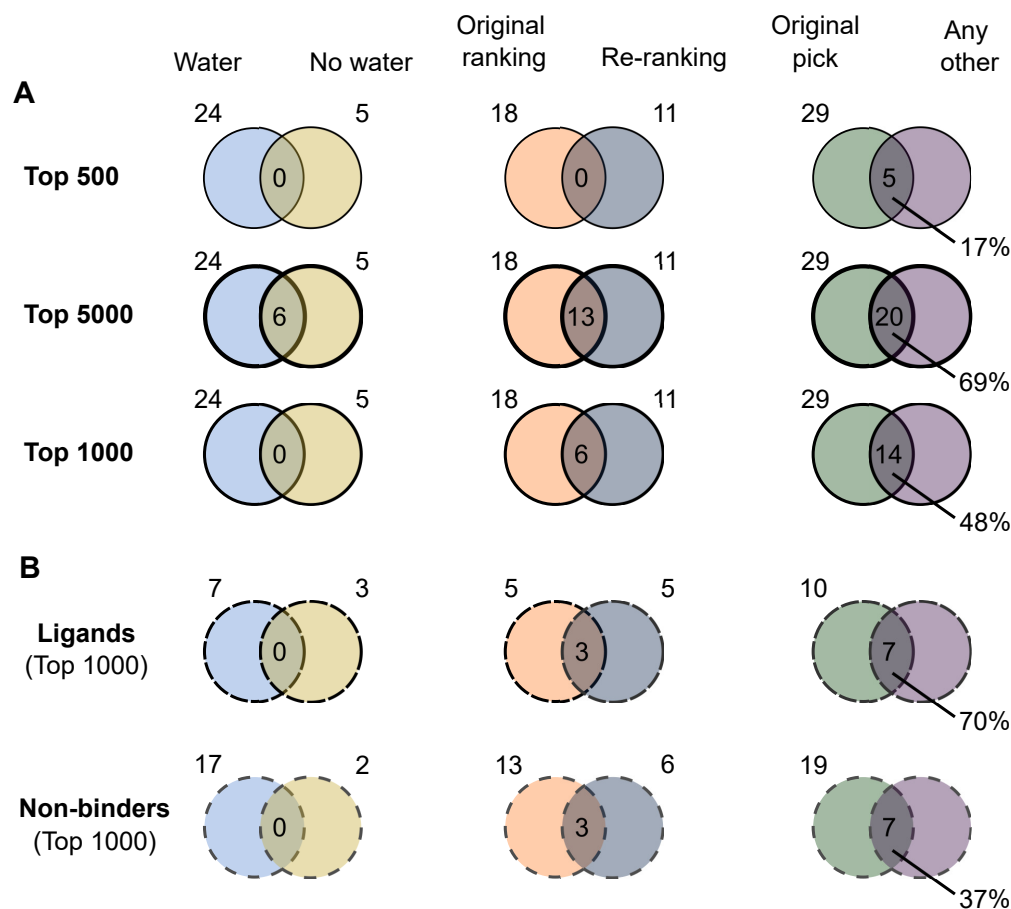


Figure 6: Venn diagrams indicating the overlap between different ranking lists. A: Comparison whether any of the molecules selected in the primary screen would have been found in another ranking list for the top 500, 5000 or 1000 ranked molecules. B: Same as in A, but considering only ligands with a $pK_i > 5$ (top) or non-binding/low affinity molecules (bottom) for the top 1000 ranked molecules. The compared ranking lists are water-containing and corresponding water-free setup (left); re-ranking and corresponding original rankings (middle; considering only re-rankings used during the docking screen); original ranking and any other ranking list (right; including water-free re-dockings). Numbers above the circle indicate how many molecules were selected from a respective ranking list. Numbers in the intersection of the circles indicate the number of individual molecules that was found in both compared sets of ranking lists. The sequence of the lines in panel A is intentional, to allow a more direct comparison with panel B.

Recommendations for future GPCR docking screens

In this study, we used different docking setups, based on a variety of CB₂R structures, to retrieve diverse – and a potentially higher number of – ligands targeting this receptor.

When comparing the ranks of the selected molecules between the different docking setups, it turned out that the overlap between the lists of top-ranked molecules is smaller than might initially have been expected. This confirms that small variations in the binding pocket of a protein, such as the insertion of a water molecule or the use of a slightly different conformation (e.g. an inactive versus an active receptor conformation), can influence docking results quite drastically.

Overall, ligands were more likely to appear in the top ranks of two or more ranking lists compared to non-binding or low-affinity molecules. Putting this observation to use, one could compare ranking lists after docking the same molecular library to two different docking setups of the same receptor to enrich ligands. This can also be achieved with a ‘dual’ re-ranking to combine two ranking lists in order to enrich molecules ranking highly in both lists. We observed that one is more likely to find a ligand than a non-binding molecule in the top ranks of both re-ranking and corresponding single ranking lists and, moreover, re-ranking improved chances to find ligands from a docking screen.

The prediction of potential water binding sites has been used as a strategy to make the hydrophobic binding site of the CB₂R more “dockable”, i.e. more suitable for successful docking screens. We note that the predicted and selected water sites within the CB₂R binding site overlap with previous suggestions for the CB₁R. (26, 27) Water molecules, when present, had a positive impact on docking poses in general, but more so for ligands than non-binders. Hence, we suggest that the introduction of water molecules to a hydrophobic binding site can be a helpful strategy to improve docking calculations both in terms of pose quality and enrichment, which has also been described previously (e.g. ref. (31)).

Application of these concepts for the CB₂R led to a hit rate of 34% (including all ligands with a pK_i>5), which is in the upper range for docking screens to GPCRs. (32) Furthermore, three of the discovered ligands have high affinities to the CB₂R with pK_i>6. Especially the ligand series based on MS022 holds promise, revealing several ligands with low similarity to previously described ligands of the CB₂R and high affinities in the same range as of SR-144,528.

Moreover, it is notable that antagonist/inverse agonist MS009 was picked from the docking calculation to a CB₂R structure in an inactive conformation, and partial agonists MS021 and MS022 were picked from docking calculations of the receptor in active conformations. This aligns with previous studies where ligands with certain efficacy values were derived from GPCR structures in corresponding conformations in docking screens. (3, 33, 34) We

note that such a one-to-one relationship of receptor conformation and ligand efficacy is not always the case, however. (35) Still, when available, considering receptor conformations corresponding to different activation states can enhance the variety of ligands in terms of efficacy.

All in all, these results and comparisons exemplify that (1) the usage of several different docking setups – for example using different receptor structures, introducing water molecules into the binding site or using different template ligands for docking calculations – can aid in finding a wider variety of ligands; (2) comparing the ranking lists resulting from these different docking setups and favouring molecules that are ranked well in more than one of them improves enrichment of ligands in the top ranks; and (3) using predicted water sites to introduce water molecules into the binding site can improve docking results, especially when dealing with hydrophobic binding sites.

Methods

In silico methods

Structure preparation. Three structures of the CB₂R with PDB IDs 5ZTY, (36) 6PT0 (37) and 6KPF (38) were prepared for docking. Missing protein side chains were modelled using the Dunbrack rotamer library in UCSF Chimera. (39, 40) For the water-free docking setups, the structures were protonated and positions of hydrogen atoms and all modelled side chains were energy-minimised using the CHARMM22 force field (41) prior to further preparation for DOCK as described below.

To explore the binding site of structure 5ZTY (defined by all residues within 8 Å distance of the ligand) a library of small fragments was docked using SEED (Solvation Energy for Exhaustive Docking; v.3.3.4). (42) The docking poses of methanol and ethanol were then visually inspected to identify polar hot spots in the binding site. For each of the selected structures (PDB IDs 5ZTY, 6PT0 and 6KPF), water binding sites were predicted using MOE's Solvent Analysis tool (which is based on the three-dimensional reference interaction site model (3D-RISM) (43); Molecular Operating Environment (MOE), 2019.01, Chemical Computing Group ULC, Montreal, Canada, 2020.) as well as OpenEye SZMAP (SZMAP 1.6.7.3. OpenEye, Cadence Molecular Sciences, Santa Fe, NM. <http://www.eyesopen.com>. (2013)). Water sites were selected based on the following: (1) favourable predicted energies; (2) their location within the binding site and in proximity to potential binding ligands and; (3) common predictions from both prediction tools. Furthermore, the selected water sites in structure 5ZTY were used as a reference to guide the selection of water sites in the other two structures. The structures were then prepared with water molecules in the selected water sites. The protein, as well as the ligands and water molecules, were protonated at pH 6-8. All hydrogen atoms, modelled side chains and water molecules together with the ligands and nearby residues in the binding site were minimised using the CHARMM22 force field.

All minimised structures were then prepared for DOCK3.7 by generating grids and spheres. In DOCK, the spheres are used to translate and rotate molecules in the binding pocket and were in some cases moved manually to optimise docking results. Furthermore, in the case of structure 5ZTY, a truncated version of ligand AM841 from the CB₁R structure with PDB ID 5XR8 (44) was used as an alternative template ligand for sphere generation, by placing it in the CB₂R binding site by aligning structures 5ZTY and 5XR8 and copying the respective ligand.

Selection of docking setups. To select among the diverse docking setups including water molecules in the different predicted sites, a set of 33 known CB₂R ligands (including the ligands from the experimental structures), were docked to each of the prepared structures

using DOCK3.7. (45) Poses were evaluated visually based on polar and apolar interactions and overall ligand orientation. Finally, docking setups yielding the highest amount of acceptable poses were selected for docking screens. Five setups thus remained for further docking calculations: 5ZTY_{H₂O} (water molecule close to S285^{7x38}), 5ZTY_{AM841} (alternative template ligand truncated-AM841 and a water molecule close to residue S285^{7x38}), 6PT0 (no water), 6PT0_{H₂O} (water molecule close to S285^{7x38}) and 6KPF_{H₂O} (two water molecules close to S285^{7x38} and L182^{ECL2}, respectively).

Docking screens and molecule selection. The docking screens were conducted as described previously, and more details can be found in the Supplementary Information. Information on compound rank comparison can also be found in the Supplementary Information.

Materials

Reagents used in cell culture and molecular biology are listed in Supplementary Table S13 and all reference compounds in Supplementary Table S14.

All tested compounds selected from the docking screens were purchased from Enamine or MolPort with $\geq 90\%$ purity. A list of identifiers, vendors and smiles can be found in Supplementary Tables S15 and S16.

Experimental methods

Cell culture and cell line production. A complete description of cell culture methods, cell membrane preparations and compound testing protocols is described in the Supplementary Information. Cell lines were established according to a protocol elsewhere. (46).

Determination of affinity constants (K_i). The affinity of CB₂R-specific ligands was determined using competition binding assays conducted in white 384-well Optiplate plates, using Hanks Balanced Salt Solution (HBSS) assay buffer (5mM HEPES, 0.5 % BSA, 0.02 % pluronic F-127 pH 7.4, and 100 μ M GppNHp).

1 μ g HEK293TR-expressing human CB₁R or CB₂R cell membrane preparations were added to each well in the assay plate, containing increasing concentrations of test compounds up to 30 μ M, in the presence of a fixed concentration of D77 fluorescent ligand (900 nM CB₁R and 900 nM CB₂R), a concentration approximately 2 \times its K_d in 50 μ L of assay buffer containing 2 % DMSO in a 384-well plate incubated at 37 °C with orbital mixing. The extent of fluorescent ligand binding to the receptor was assessed at 60 min by HTRF detection. Non-specific binding was determined as the amount of HTRF signal detected in the presence of either SR-144,528, 10 μ M or rimonabant, 10 μ M and was subtracted from total binding, to calculate specific binding, meaning that $t=0$ was always equal to zero. Steady-state

competition binding was obtained after incubating the plate for 60 min prior to reading the plate.

Mini-G protein and β -arrestin recruitment assays in CB₂R-expressing cells.

CB₂R coupling to G proteins was assessed using a fluorescent G protein surrogate, venus-mini-G_{si1} (vmG_{si}) protein. (47) The venus-mG_{si} subunit is a chimeric protein consisting of C-terminal G_{i1} residues grafted onto venus-mG_s, which was originally engineered from the native G_{os} protein. The venus-mG_{si} is useful for studying receptor activation of the CB₂R, as unlike its wild type G_{oi1} counterpart, the resulting active-receptor complex formed is stable and resistant to nucleotide exchange. Thus, active-state signalling is maintained if the agonist is present.

HEK293TR-CB₂R-nLuc stable cell lines expressing fluorescently-labelled miniG or β -arrestin protein were maintained according to the cell culture protocols outlined in the Supplementary Information. Following a 48hr incubation after plating the cells and inducing CB₂R expression, the cell culture media was aspirated, and the cells were washed in 100 μ L/well assay buffer (HBSS, 0.5 % BSA, 5 mM HEPES). 90 μ L/well assay buffer containing 10 μ M flurimazine, was applied to each well. The plate was then sealed and incubated for 15 min at 37 °C to allow flurimazine to enter the cells. Test compounds were prepared via serial dilutions in DMSO and then in assay buffer. Finally, 10 μ L of compounds were then added to the plate following the initial baseline reading, and the plate was read for 30 min.

G_i-CASE assay. Gi-CASE assays were performed similarly to those described in Scott-Dennis *et al.* (48) Compound profiling in the membrane-based CB₁R and CB₂R G_i-CASE system used a HBSS assay buffer (0.02 % pluronic F127, 0.5 % BSA, 5 mM HEPES), using the reference compounds HU-210, SR-144,528 and the test compounds serially diluted in DMSO in a Greiner 96-well plate, and transferred to the 384-well OptiplatTM (PerkinElmer). Finally, the CB₂R membrane preparations expressing the G_i-CASE biosensor were diluted in assay buffer containing 50 μ M flurimazine, before adding to the assay plate at 5 μ g/well and reading for 1hr.

Signal Detection and Data Analysis. All pharmacological assays were performed on a PHERAstar FSX (BMG Labtech, Offenburg, Germany). For TR-FRET assays, the terbium donor was excited with four laser flashes at a wavelength of 337 nm. TR-FRET signals were then collected at 520nm (acceptor) and 620 nm (donor surrogate), when using the green NBD-containing fluorescent ligand D77. (46) TR-FRET ratios were obtained by dividing the acceptor signal by the donor signal and multiplying this value by 10 000. Data from the TR-FRET assays was fitted using GraphPad Prism 9.2 to the one-site competition binding model (Equation 2) to calculate IC₅₀ values, which were converted to K_i values by applying the Cheng-Prusoff correction (see Supplementary Information).

The miniG or β -arrestin recruitment assays were carried out at 37 °C, and included three BRET cycles to obtain a baseline reading before adding the test compounds to the plate. Gi-CASE membrane assays were carried out at 28 °C using a BRET1 plus module (535-30LP/475-30BP). The vehicle control was assay buffer containing 10 % DMSO (1 % final), and all responses were normalised to the maximal response produced by either HU-210 or HU-308 depending on the CB receptor. Assay data were processed in Microsoft Excel and analysed in GraphPad PRISM 9.2 (GraphPad Software, San Diego, USA).

A complete description of data analysis and handling methods is provided in the Supplementary Information.

Contributions

Project was designed by M.M.S. and P.K. Computational studies were performed by M.M.S. and F.N.Z.G. Pharmacological assays and data analysis was done by M.S.-D., L.B.-R., D.P., and D.A.S. Data was analysed by M.M.S. and P.K. Manuscript was written and edited by all authors. Project was supervised by D.B.V. and P.K.

Acknowledgements

The authors thank Dr Bianca Casella and Dr Shailesh Mistry at the University of Nottingham UK for their help with the quality control of all assayed compounds. The work was supported by grants from the German Research Foundation (DFG; MMS: 470002134, PK: KO4095/3-1, KO4095/4-1 and KO4095/5-1), and Svenska Sällskapet för Medicinsk Forskning (SSMF; MMS: PG-22-0379). LBR is a recipient of a Predoctoral grant awarded by the Department of Education of the Basque Government, a Short-Term Fellowship awarded by European Molecular Biology Organization (EMBO) and a Short-Term Scientific Mission grant awarded by European Research Network on Signal Transduction (ERNEST, COST Action 18133). DAS and DBV gratefully acknowledge funding by F. Hoffmann-La Roche Ltd., Basel, Switzerland [Roche Postdoctoral Fellowship RPF-551]. DBV gratefully acknowledges funding by the Swiss National Science Foundation grants 135754 and 159748 and the Novartis Foundation FreeNovation grant. DAS and DBV gratefully acknowledge funding by the Medical Research Council [grant number MR/Y003667/1]. MSD is funded by the Biotechnology and Biological Sciences Doctoral Training Programme at the University of Nottingham. MMS, PK, LBR, MSD, DAS, and DBV were members of COST Action CA18133 “ERNEST”.

Funding sources

The work was supported by grants from the German Research Foundation (DFG; MMS: 470002134, PK: KO4095/3-1, KO4095/4-1 and KO4095/5-1), and Svenska Sällskapet för Medicinsk Forskning (SSMF; MMS: PG-22-0379). LBR is a recipient of a Predoctoral grant awarded by the Department of Education of the Basque Government, a Short-Term Fellowship awarded by European Molecular Biology Organization (EMBO) and a Short-Term Scientific Mission grant awarded by European Research Network on Signal Transduction (ERNEST, COST Action 18133). DAS and DBV gratefully acknowledge funding by F. Hoffmann-La Roche Ltd., Basel, Switzerland [Roche Postdoctoral Fellowship RPF-551].

DBV gratefully acknowledges funding by the Swiss National Science Foundation grants 135754 and 159748 and the Novartis Foundation FreeNovation grant. DAS and DBV gratefully acknowledge funding by the Medical Research Council [grant number MR/Y003667/1]. MSD is funded by the Biotechnology and Biological Sciences Doctoral Training Programme at the University of Nottingham.

Conflicts of Interest

D.A.S. and D.B.V. are founding directors of Z7 Biotech Ltd, an early-stage drug discovery company. All other authors declare no conflict of interest.

Supplementary Information

Supplementary Results are online at. . .

References

- (1) Schmidt, D., Bernat, V., Brox, R., Tschammer, N., and Kolb, P. (2015). Identifying Modulators of CXC Receptors 3 and 4 with Tailored Selectivity using Multi-Target Docking. *ACS Chem. Biol.* *10*, 715–724.
- (2) Matricon, P., Nguyen, A. T., Vo, D. D., Baltos, J.-A., Jaiteh, M., Lutgens, A., Kampen, S., Christopoulos, A., Kihlberg, J., May, L. T., and Carlsson, J. (2023). Structure-based virtual screening discovers potent and selective adenosine A1 receptor antagonists. *Eur. J. Med. Chem.* *257*, 115419.
- (3) Scharf, M. M., Bünemann, M., Baker, J. G., and Kolb, P. (2019). Comparative Docking to Distinct G Protein-Coupled Receptor Conformations Exclusively Yields Ligands with Agonist Efficacy. *Mol. Pharmacol.* *96*, 851–861.
- (4) Kirchhofer, S. B., Lim, V. J. Y., Ernst, S., Karsai, N., Julia, R. G., Canals, M., Kolb, P., and Bünemann, M. (2023). Differential interaction patterns of opioid analgesics with μ opioid receptors correlate with ligand-specific voltage sensitivity. *eLife* *12*, e91291.
- (5) Köck, Z., Schnelle, K., Persechino, M., Umbach, S., Schihada, H., Janulienė, D., Parey, K., Pockes, S., Kolb, P., Dötsch, V., Möller, A., Hilger, D., and Bernhard, F. (2024). Cryo-EM structure of cell-free synthesized human histamine 2 receptor/Gs complex in nanodisc environment. *Nat. Commun.* *15*, 1831.
- (6) Auvity, S., Attili, B., Caillé, F., Goislard, M., Cayla, J., Hinnen, F., Demphel, S., Brulon, V., Bottlaender, M., Leroy, C., Bormans, G., Kuhnast, B., and Peyronneau, M. A. (2024). Translational Preclinical PET Imaging and Metabolic Evaluation of a New Cannabinoid 2 Receptor (CB2R) Radioligand, (Z)-N-(3-(2-(2-[18F]Fluoroethoxy)ethyl)-4,5-dimethylthiazol-2(3H)-ylidene)-2,2,3,3-tetramethylcyclopropane-1-carboxamide. *ACS Pharmacol. Transl. Sci.* *7*, 3144–3154.
- (7) Pacher, P., and Kunos, G. (2013). Modulating the endocannabinoid system in human health and disease – successes and failures. *FEBS J.* *280*, 1918–1943.
- (8) Pertwee, R. G. (1997). Pharmacology of cannabinoid CB1 and CB2 receptors. *Pharmacol. Ther.* *74*, 129–180.
- (9) Atwood, B. K., and MacKie, K. (2010). CB 2: A cannabinoid receptor with an identity crisis. *Br. J. Pharmacol.* *160*, 467–479.
- (10) Mallat, A., Teixeira-Clerc, F., and Lotersztajn, S. (2013). Cannabinoid signaling and liver therapeutics. *J. Hepatol.* *59*, 891–896.

- (11) Mukhopadhyay, P., Rajesh, M., Pan, H., Patel, V., Mukhopadhyay, B., Bátkai, S., Gao, B., Haskó, G., and Pacher, P. (2010). Cannabinoid-2 receptor limits inflammation, oxidative/nitrosative stress, and cell death in nephropathy. *Free Radic Biol Med* 48, 457–467.
- (12) Mukhopadhyay, P. et al. (2016). The novel, orally available and peripherally restricted selective cannabinoid CB2 receptor agonist LEI-101 prevents cisplatin-induced nephrotoxicity. *Br. J. Pharmacol.* 173, 446–458.
- (13) Wright, K. L., Duncan, M., and Sharkey, K. A. (2008). Cannabinoid CB2 receptors in the gastrointestinal tract: a regulatory system in states of inflammation. *Br. J. Pharmacol.* 153, 263–270.
- (14) Ofek, O., Karsak, M., Leclerc, N., Fogel, M., Frenkel, B., Wright, K., Tam, J., Attar-Namdar, M., Kram, V., Shohami, E., Mechoulam, R., Zimmer, A., and Bab, I. (2006). Peripheral cannabinoid receptor, CB2, regulates bone mass. *Proc. Natl. Acad. Sci. U. S. A.* 103, 696–701.
- (15) Grabon, W., Ruiz, A., Gasmi, N., Degletagne, C., Georges, B., Belmeguenai, A., Bodennec, J., Rheims, S., Marcy, G., and Bezin, L. (2024). CB2 expression in mouse brain: from mapping to regulation in microglia under inflammatory conditions. *J Neuroinflammation* 21, 206.
- (16) Aebi, J. et al. (2024). Enhancing Drug Discovery and Development through the Integration of Medicinal Chemistry, Chemical Biology, and Academia-Industry Partnerships: Insights from Roche’s Endocannabinoid System Projects. *CHIMIA* 78, 499–512.
- (17) Grabon, W., Rheims, S., Smith, J., Bodennec, J., Belmeguenai, A., and Bezin, L. (2023). CB2 receptor in the CNS: From immune and neuronal modulation to behavior. *Neurosci. Biobehav. Rev.* 150, 105226.
- (18) Vuic, B., Milos, T., Tudor, L., Konjevod, M., Nikolac Perkovic, M., Jazvinscak Jembrek, M., Nedic Erjavec, G., and Svob Strac, D. (2022). Cannabinoid CB2 Receptors in Neurodegenerative Proteinopathies: New Insights and Therapeutic Potential. *Biomedicines* 10, 3000.
- (19) Kosar, M. et al. (2024). Flipping the GPCR Switch: Structure-Based Development of Selective Cannabinoid Receptor 2 Inverse Agonists. *ACS. Cent. Sci.* 10, 956–968.

- (20) Sarsembayeva, A., Kienzl, M., Gruden, E., Ristic, D., Maitz, K., Valadez-Cosmes, P., Santiso, A., Hasenoehrl, C., Brcic, L., Lindenmann, J., Kargl, J., and Schicho, R. (2023). Cannabinoid receptor 2 plays a pro-tumorigenic role in non-small cell lung cancer by limiting anti-tumor activity of CD8+ T and NK cells. *Front. Immunol.* *13*, 997115.
- (21) Sarsembayeva, A., and Schicho, R. (2023). Cannabinoids and the endocannabinoid system in immunotherapy: helpful or harmful? *Front. Oncol.* *13*, 1296906.
- (22) Spinelli, F., Capparelli, E., Abate, C., Colabufo, N. A., and Contino, M. (2017). Perspectives of Cannabinoid Type 2 Receptor (CB2R) Ligands in Neurodegenerative Disorders: Structure-Affinity Relationship (SAfiR) and Structure-Activity Relationship (SAR) Studies. *J. Med. Chem.* *60*, 9913–9931.
- (23) Xiang, W. et al. (2018). Monoacylglycerol lipase regulates cannabinoid receptor 2-dependent macrophage activation and cancer progression. *Nat. Commun.* *9*, 2574.
- (24) Stasiulewicz, A., Lesniak, A., Bujalska-Zadrożny, M., Pawiński, T., and Sulkowska, J. I. (2023). Identification of Novel CB2 Ligands through Virtual Screening and In Vitro Evaluation. *J. Chem. Inf. Model.* *63*, 1012–1027.
- (25) Isberg, V., de Graaf, C., Bortolato, A., Cherezov, V., Katritch, V., Marshall, F. H., Mordalski, S., Pin, J.-P., Stevens, R. C., Vriend, G., and Gloriam, D. E. (2015). Generic GPCR residue numbers - aligning topology maps while minding the gaps. *Trends Pharmacol. Sci.* *36*, 22–31.
- (26) Kumar, K. K. et al. (2019). Structure of a Signaling Cannabinoid Receptor 1-G Protein Complex. *Cell* *176*, 448–458.e12.
- (27) Díaz, Ó., Dalton, J. A., and Giraldo, J. (2019). Revealing the Mechanism of Agonist-Mediated Cannabinoid Receptor 1 (CB1) Activation and Phospholipid-Mediated Allosteric Modulation. *J. Med. Chem.* *62*, 5638–5654.
- (28) McAllister, S. D., Hurst, D. P., Barnett-Norris, J., Lynch, D., Reggio, P. H., and Abood, M. E. (2004). Structural mimicry in class A G protein-coupled receptor rotamer toggle switches: The importance of the F3.36(201)/W6.48(357) interaction in cannabinoid CB1 receptor activation. *J. Biol. Chem.* *279*, 48024–48037.
- (29) Filipek, S. (2019). Molecular switches in GPCRs. *Curr. Opin. Struct. Biol.* *55*, 114–120.

- (30) Manera, C., Saccomanni, G., Adinolfi, B., Benetti, V., Ligresti, A., Cascio, M. G., Tucinardi, T., Lucchesi, V., Martinelli, A., Nieri, P., Masini, E., Di Marzo, V., and Ferrarini, P. L. (2009). Rational design, synthesis, and pharmacological properties of new 1,8-naphthyridin-2(1H)-on-3-carboxamide derivatives as highly selective cannabinoid-2 receptor agonists. *J. Med. Chem.* *52*, 3644–3651.
- (31) Roberts, B. C., and Mancera, R. L. (2008). Ligand-Protein Docking with Water Molecules. *J. Chem. Inf. Model.* *48*, 397–408.
- (32) Ballante, F., Kooistra, A. J., Kampen, S., Graaf, C. D., and Carlsson, J. (2021). Structure-Based Virtual Screening for Ligands of G Protein-Coupled Receptors : What Can Molecular Docking Do for You? *Pharmacol. Rev.* *73*, 527–565.
- (33) Weiss, D. R., Ahn, S., Sassano, M. F., Kleist, A., Zhu, X., Strachan, R., Roth, B. L., Lefkowitz, R. J., and Shoichet, B. K. (2013). Conformation Guides Molecular Efficacy in Docking Screens of Activated β -2 Adrenergic G Protein Coupled Receptor. *ACS Chem. Biol.* *8*, 1018–1026.
- (34) Kooistra, A. J., Vischer, H. F., McNaught-Flores, D., Leurs, R., de Esch, I. J. P., and de Graaf, C. (2016). Function-specific virtual screening for GPCR ligands using a combined scoring method. *Sci. Rep.* *6*, 28288.
- (35) Papadopoulos, M. G. E., Perhal, A. F., Medel-Lacruz, B., Ladurner, A., Selent, J., Dirsch, V. M., and Kolb, P. (2024). Discovery and characterization of small-molecule TGR5 ligands with agonistic activity. *Eur. J. Med. Chem.* *276*, 116616.
- (36) Li, X. et al. (2019). Crystal Structure of the Human Cannabinoid Receptor CB2. *Cell* *176*, 459–467.e13.
- (37) Xing, C. et al. (2020). Cryo-EM Structure of the Human Cannabinoid Receptor CB2-Gi Signaling Complex. *Cell* *180*, 645–654.e13.
- (38) Hua, T. et al. (2020). Activation and Signaling Mechanism Revealed by Cannabinoid Receptor-Gi Complex Structures. *Cell* *180*, 655–665.e18.
- (39) Shapovalov, M. V., and Dunbrack, R. L. (2011). A smoothed backbone-dependent rotamer library for proteins derived from adaptive kernel density estimates and regressions. *Structure* *19*, 844–858.
- (40) Pettersen, E. F., Goddard, T. D., Huang, C. C., Couch, G. S., Greenblatt, D. M., Meng, E. C., and Ferrin, T. E. (2004). UCSF Chimera—A visualization system for exploratory research and analysis. *J. Comput. Chem.* *25*, 1605–1612.
- (41) Momany, F. A., and Rone, R. (1992). Validation of the general purpose QUANTA 3.2/CHARMm force field. *J. Comput. Chem.* *13*, 888–900.

- (42) Majeux, N., Scarsi, M., Apostolakis, J., Ehrhardt, C., and Caffisch, A. (1999). Exhaustive Docking of Molecular Fragments With Electrostatic Solvation. *Proteins: Struct., Funct., Bioinf.* 37, 88–105.
- (43) Beglov, D., and Roux, B. (1997). An integral equation to describe the solvation of polar molecules in liquid water. *J. Phys. Chem. B* 101, 7821–7826.
- (44) Hua, T. et al. (2017). Crystal structures of agonist-bound human cannabinoid receptor CB1. *Nature* 547, 468–471.
- (45) Coleman, R. G., Carchia, M., Sterling, T., Irwin, J. J., and Shoichet, B. K. (2013). Ligand Pose and Orientational Sampling in Molecular Docking. *PLoS one* 8, e75992.
- (46) Borrega-Roman, L. et al. (2024). A universal cannabinoid CB1 and CB2 receptor TR-FRET kinetic ligand binding assay. *bioRxiv*, 2024.07.16.603654.
- (47) Wan, Q., Okashah, N., Inoue, A., Nehmé, R., Carpenter, B., Tate, C. G., and Lambert, N. A. (2018). Mini G protein probes for active G protein–coupled receptors (GPCRs) in live cells. *J. Biol. Chem.* 293, 7466–7473.
- (48) Scott-Dennis, M., Rafani, F. A., Yi, Y., Perera, T., Harwood, C. R., Guba, W., Rufer, A. C., Grether, U., Veprintsev, D. B., and Sykes, D. A. (2023). Development of a membrane-based Gi-CASE biosensor assay for profiling compounds at cannabinoid receptors. *Front. Pharmacol.* 14, DOI: 10.3389/fphar.2023.1158091.